ILASS 2008
Sep. 8-10, 2008, Como Lake, Italy

Paper ID ILASS08-2-14

SIMULATION OF THE FILM FORMATION AT A HIGH-SPEED ROTARY BELL ATOMIZER USED IN AUTOMOTIVE SPRAY PAINTING PROCESSES

J. Domnick*, Z. Yang ° and Q. Ye °

* Esslingen University of Applied Sciences, Kanalstr. 33, 73728 Esslingen, Germany
° Fraunhofer-Institute for Manufacturing Engineering and Automation
Nobelstr. 12, 70569 Stuttgart, Germany

ABSTRACT

The present contribution summarizes investigations aiming to calculate the two phase flow field inside the manifold of a rotary bell atomizer and the free film on the rotary bell surface. Calculations are based on the CFD code Fluent using the Volume of Fluid (VOF) method. The phase distribution in the bell's manifold as well as the film thickness on the bell was determined, the latter result being compared with an analytical solution also. The simulations were carried out on a CRAY-Opteron Cluster available at the Hochleistungsrechenzentrum HLRS of the University of Stuttgart. It was found that the paint flow is emerging from the paint nozzle forming a relatively thick film on the so-called distributor disk. The blockage of the distributor disk mount (3 separate bolts) leads to a paint flow from the distributor disk to the inner surface of the bell. The major paint fraction, however, leaves the distributor surface at the edge of the horizontal channel, further flowing along the bell surface towards the bell edge. However, finally a stable film is formed on the bell surface. Here, the estimated film thicknesses from the VOF simulations coincide very well with results from an analytical solution. Consequently, bubble formation in the paint, which is one of the reasons for these investigations, can only take place in the mixing zone between paint nozzle exit and distributor disk, where the paint jet impacts on the distributor disk surface. In the future, the investigations will be extended to calculate jet formation and disintegration.

INTRODUCTION

High-speed rotary bell atomizers are widely used in the painting industry for high quality applications. In some applications using novel paint materials, however, small gas bubbles can be observed in the wet paint film on the substrates, resulting in a decreasing overall painting quality, sometimes requiring also manual repairs. It was found that this bubble occurrence depends on the specific paints materials, the geometry of the rotating bells as well as the chosen operating parameters of the atomizer. Clearly, some fundamental research, e.g., studies concerning the paint flow inside the atomizer and on the bell's surface should be carried out in order to assist a future physical explanation of the bubble problem mentioned above.

In general, some work dealing with rotary atomizers has been done to examine the atomization processes [1, 2]. *Domnick* et al. have presented results for a high-speed rotary atomizer used for painting applications applying water-based non Newtonian liquid paints. In their experimental work, the rheological characterization of the paint, the visualization of the disintegration process as well as the measurement of droplet size has been carried out. The measured droplet size distribution was further applied into their numerical simulation of the spray painting process considering also the effects of electrostatic field and charged paint droplets [2, 3]. The final film thickness on the target and the transfer efficiency could be estimated.

Until now there are only a few research publications in public literature concerning the paint flow inside rotary bell atomizers available. Especially the flow field inside the atomizer's manifold as the origin of the developing free film on the bell's surface is not well understood. Experimental investigations in this region are quite difficult due to the small dimensions and the high speed bell rotation up to 60 000 1/min. Hence, numerical simulations provide an appropriate alternative, since the initial flow conditions and the required boundary conditions can be derived from overall atomizer parameters easily.

The present contribution summarizes investigations aiming to calculate the two phase flow field inside the manifold of a rotary bell atomizer and the free film on the rotary bell surface. Calculations are based on the CFD code Fluent using the Volume of Fluid (VOF) method. The phase distribution in the bell's manifold as well as the film thickness on the bell was determined, the latter result being compared with an analytical solution also.

CHARACTERISTICS OF THE ATOMIZER

The investigations shown here were made with a state-of-the-art high-speed rotary bell atomizer (Dürr Systems GmbH) used in automated paint applications. A front view of the atomizer is depicted in Fig. 1. Fig. 2 shows a cross section of the bell, basically consisting of an inner distributor disk and the bell itself. The purpose of the distributor disk is to evenly distribute the paint emerging from a central nozzle (diameter 1.3 mm) on the inner bell surface.

The paint supply nozzle is surrounded by an annular slit with a width of 0.34 mm, through which ambient air is sucked in. Bell and distributor disk are assembled together by three spikes. During operation both the bell and the distributor disk rotate at high speed, while the nozzle for paint supply remains static. Applying paint through the nozzle, a paint film is formed on the centre of the distributor disk's backside, which is further radially accelerated by centrifugal forces and eventually becomes unstable at a certain distance from the rotating axis. Finally, the paint becomes distributed on the distributor disk surface as well as the bell surface itself.

Figure 1: Front view of the rotary bell atomizer

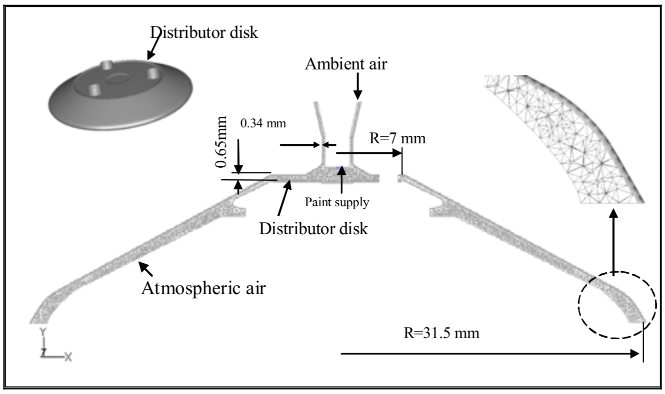

Figure 2: Cross section of the bell

In Table 1, the major characteristics of the atomizer and the operating conditions used in the simulations are summarized. Operating conditions and fluid properties are typical for the application of clear coat paint used in the automotive industry. The viscosity of solvent borne clear coat has Newtonian characteristics.

Bell diameter	63 mm
Bell Material	Stainless Steel
Bell speed	40 000, 60 000 1/min
Liquid flow rate	550 ml/min
Viscosity of liquid	0.086 Pa s
Surface tension	0.03 N/m

Table 1: Atomizer parameters used in the simulations

NUMERICAL METHOD

Due to the complicated geometry without any symmetry, a fully 3-dimensional computational domain using an unstructured grid had to be built. In addition, boundary layers with prism cells on both the bell and the distributor disk were generated. The wall cell resolution, i.e. the first interior node distance to the wall was about 10 μm, ensuring the necessary resolution for the calculation of the film thickness on the bell. The total number of cell elements was about 2 millions. Details of the numerical grid are shown in Fig. 2.

The numerical simulations presented in this work were carried out with the commercial CFD code FLUENT based on the finite-volume approach. The VOF model was used to calculate the two phase flow field and the liquid-gas interface inside the rotary bell.

The flow field and the liquid-gas interfaces are solved by the volume fraction equation and single set momentum equations:

$$\frac{1}{\rho_q}\left[\frac{\partial}{\partial t}\left(\alpha_q \rho_q\right) + \nabla \cdot \left(\alpha_q \rho_q \vec{v}_q\right) = 0\right] \tag{1}$$

$$\frac{\partial}{\partial t}\left(\rho \vec{v}\right) + \nabla \cdot \left(\rho \vec{v} \vec{v}\right) = -\nabla p + \nabla \cdot \left[\mu\left(\nabla \vec{v} + \nabla \vec{v}^{T}\right)\right] + \rho \vec{g} + \vec{F}$$

where $\vec{v}$ denotes the velocity vector, t the time, ρ the density, μ the dynamic viscosity, p the pressure and α_q the q^{th} volume fraction of the fluid in the cell. The resulting velocity field is shared among the phases.

Time-dependent VOF calculations were carried out using a typical time step of 1 μs. Since in the present work the intermediate transient flow behaviour is of major interest, an explicit interpolation scheme for solving Eq. (1) together with a geometric reconstruction scheme for the volume fraction discretization [4] was used, ensuring a sharp interface between liquid and gas phase.

The simulations presented in this paper were carried out on a CRAY-Opteron Cluster at the Hochleistungsrechen-zentrum of the University of Stuttgart. It was found that a physical time of 0.07 s was necessary to reach a quasi-stable state of the film distribution on the bell atomizer. Considering the small time step used in the simulation, the total number of time steps was 70 000. With 20 CPUs and a grid resolution of 2 million cells the computational time was approximately 500 h for one calculation case.

RESULTS AND DISCUSSION

In general, two different kinds of flow fields are present. The inner part between the distributor disk and the bell surface consists of two parallel faces almost perpendicular to the bell axis forming a relatively narrow gap (height 0.65 mm) in between. Due to the rotation of bell and distributor disk, this geometry should act like a radial pump for the liquid/air mixture.

Downstream of the edge of the distributor disk, there is a free film flow forming on the inner bell surface. This film is stabilized by the normal component of the centrifugal forces. In fact, the geometry of the bell is purposely designed to have a thin but stable film without any dewetting. As shown below, the final film thicknesses at the edge of the bell are in a range between 20 and 30 μm

Flow between distributor disk and bell

Firstly, focusing on the flow field in the channel between the bell and the distributor, the phase distribution is shown in Fig. 3. Basically, a relatively thick film is located above the distributor disk flowing around the 3 spikes. The blockage of the spikes leads to some paint flow from the distributor disk to the surface of the bell. The major paint fraction, however, detaches from the distributor surface at the edge of the horizontal channel and jumps to the bell's inner surface, further flowing along the bell surface towards the bell edge. Some paint is also able to stay attached, leaving the distributor disk surface not before its outer edge. Finally, the paint film propagates further outward towards the bell edge (not included in Fig. 2).

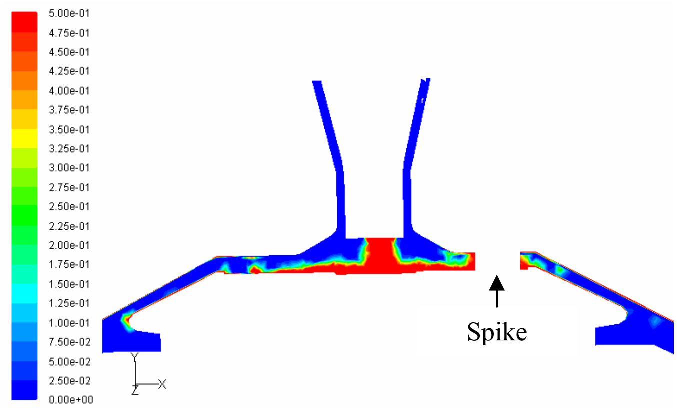

Figure 3: Contours of volume fraction of liquid in cross-section z = 0 (n = 60 000 1/min)

Figure 4 shows the velocity vectors plotted in the same cross-section as used in Fig. 3. Atmospheric air is sucked into the channel formed by the distributor disk and the bell surface, resulting in relatively high air velocities in y-direction. In the case shown here (bell speed 60 000 1/min) the maximum air inlet velocity parallel to the paint nozzle exceeds 25 m/s. Clearly, the will be a mixture zone formed between the end of the paint nozzle and the surface of the distributor disk.

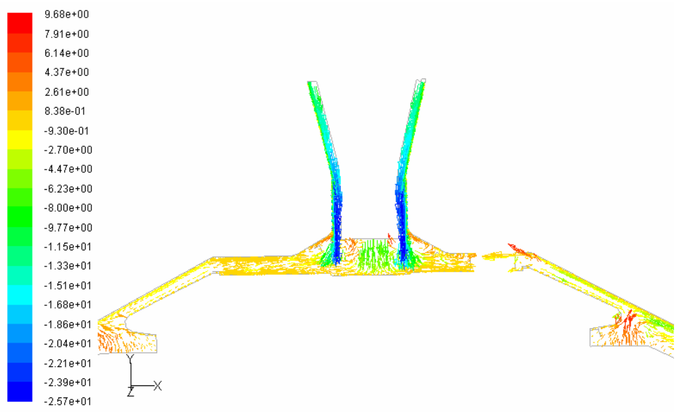

Figure 4: Velocity vector colored by the y-velocity (mixture) in cross-section z = 0 (m/s) (n = 60 000 1/min)

In the expansion region, namely from the air channel to the film channel, flow circulation is also observed; however, the volume fraction of the liquid in this region is quite low. Positive velocity component in y-direction can be seen in the corner of the horizontal film channel and in the region close to the edge of the distributor disk, corresponding to the flow circulation in these two regions.

The surface wetting on the distributor disk is depicted in Fig. 5. Considering the rotating direction of the bell and the relative movement of liquid around the spikes, small wake flow regions are obtained that are partially not wetted even in the quasi-stable state.

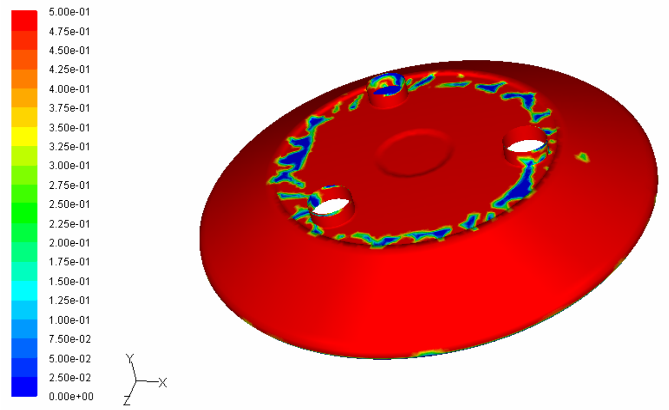

Figure 5: Contour of the liquid volume fraction on the distributor disk (color bar indicates volume fraction of liquid)

A closer look on the region between the outer edge of the distributor disk and the bell's inner surface is given by. Fig. 6. Of course, this is not more than a snapshot of an unsteady simulation. Basically, it shows that the main part of the paint flows along the surface of the distributor disk, finally detaching at the edge of the disk forming a film on the bell. However, the distributor disk surface is not completely wetted. This might be an indication for a certain instability in this region, caused by the effect of the centrifugal force.

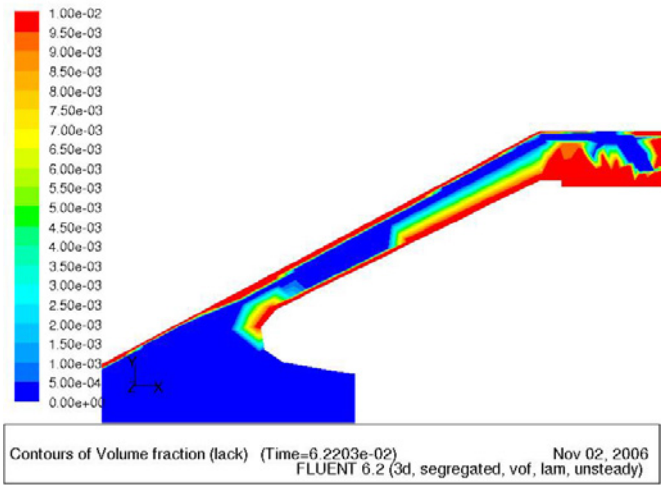

Figure 6: Phase distribution in the region between the outer edge of the distributor disk and the bell surface.

Film flow on the bell surface

In contrast to the inner surface of the distributor disk, the bell's surface is totally wetted after only approximately 8 ms, as shown in Fig. 7.

Outside the channel, i.e., free film on the rotary bell, there is constant atmospheric pressure without any further promotion of a gas release process. In the fully developed film flow situation, the film distribution on the bell surface is stable. The thickness at the bell edge, where subsequent atomization occurs, can be easily derived from the results shown in Fig. 8, with the first grid layer having a thickness of 10 µm, the second of 12 µm and the third of 14.4 µm. Hence, film thicknesses of approximately 22 µm for a rotary speed of

60 000 1/min and ca. 30 µm for a speed of 40 000 1/min are obtained.

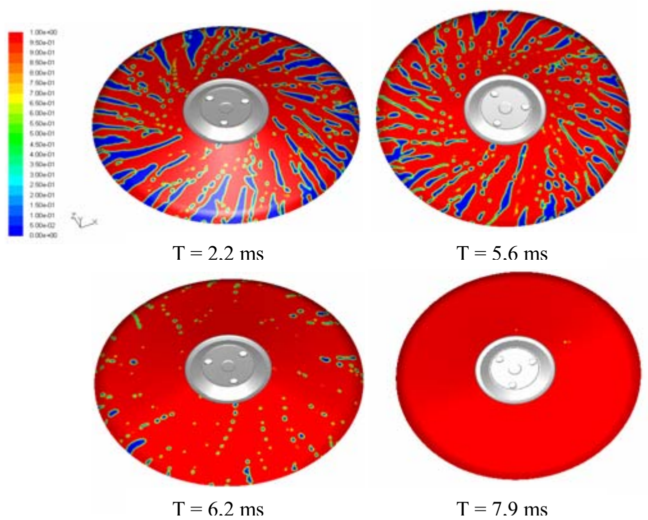

Figure 7: Visualization of the film development on the bell (color bar indicates volume fraction of liquid).

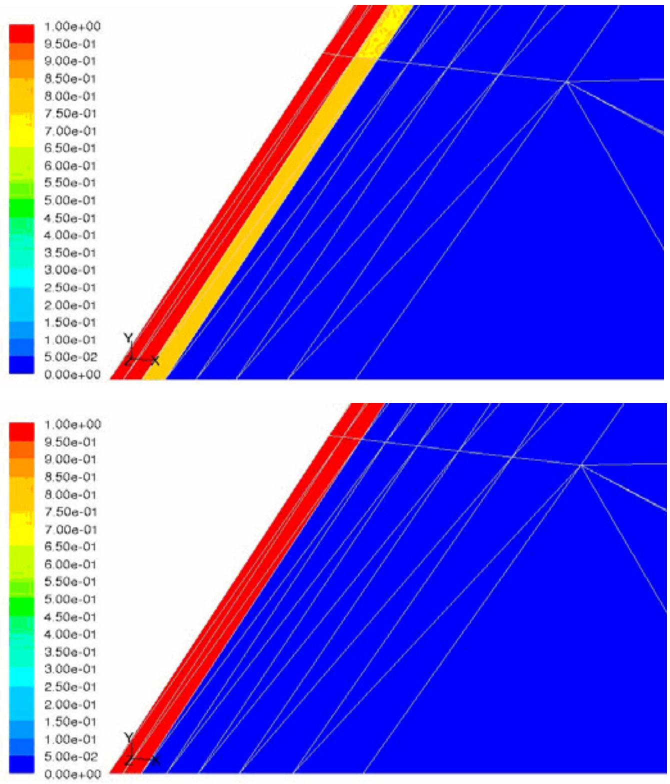

Figure 8: Contours of volume fraction (liquid) at the edge of the bell at rotary speeds of 40 000 1/min (upper) and 60 000 l/min (lower figure)

These numerically obtained film thicknesses are in reasonable agreement with an analytical solution based on an analysis of the viscose film flow at rotating disk atomizers [5]. As indicated by Fig. 9, analytical values of 27 µm for 60 000 1/min and 35 µm for 40 000 1/min are obtained. The shape of the curves basically corresponds to variations of the bell shape, as the local film thickness is strongly depending on the surface angle relative to the axis of the rotating system. The corresponding film velocities are shown in Fig. 10 with values at the bell edge being 1.7 m/s for 40 000 1/min and 1,3 m/s for 60 000 1/min. Of course, the flow can be assumed to have laminar character, as it is assumed in the numerical simulations.

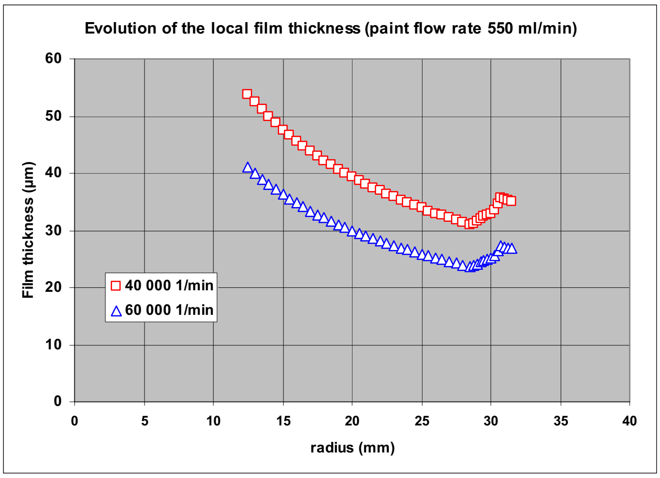

Figure. 9: Analytically calculated evolution of the local film thickness on the surface of the bell.

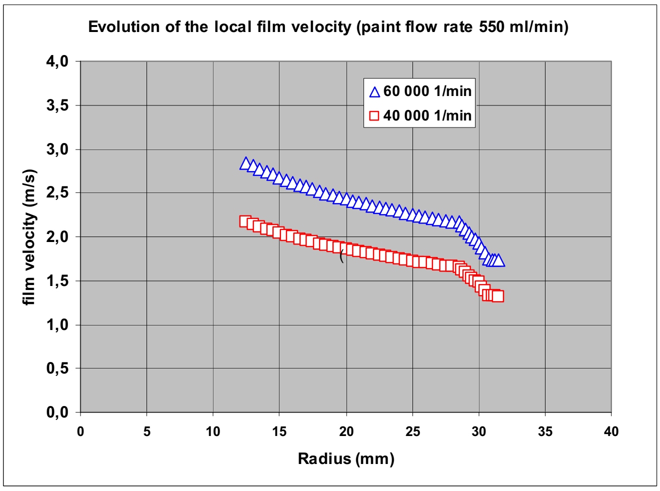

Figure. 10: Analytically calculated evolution of the local film velocity on the surface of the bell.

SOME REMARKS ON ATOMIZATION

Apart from this very specific task of detecting a potential risk for bubble formation, the results shown here may also serve as a basis for future simulations of the droplet formation. Of course, the disintegration processes is depending on the local film properties at the bell edge. Here, it must be distinguished between non-serrated and serrated bells as shown in Fig. 11.

The disintegration processes at the bell edge for a bell speed of 40 000 1/min are shown in Fig. 12 (serrated bell) and Fig. 13 (without serrations). Here, a 20 ns Nanolight system has been applied, freezing the droplet formation at the edge of the rotating bell. Obviously, well organized stable jets occur in the case of a serrated bell edge with jet lengths up to 5 to 6 mm. In contrast, the disintegration process without serrations is characterized by rather short disintegration zone with an extension of less than 1 mm around the bell. According to *Domnick* and *Thieme* [6] this may be called transition disintegration, as it is neither considered as jet nor as sheet disintegration.

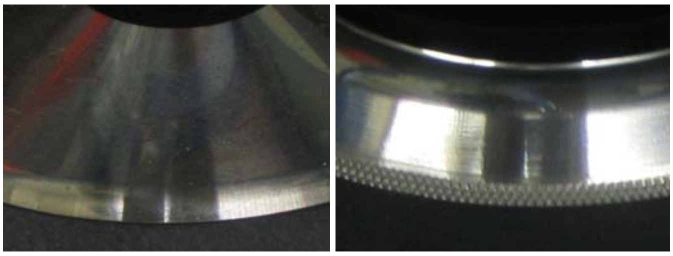

Figure 11: Details of non-serrated (left) and serrated (right) bell edges

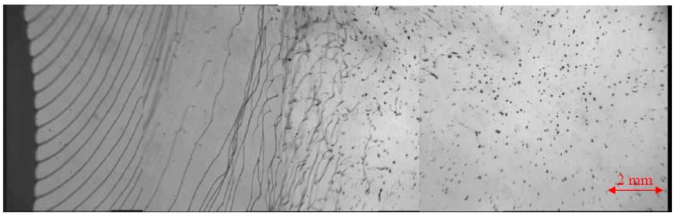

Figure 12: Jet disintegration process at bell edge (with serrations at bell edge, 40 000 1/min)

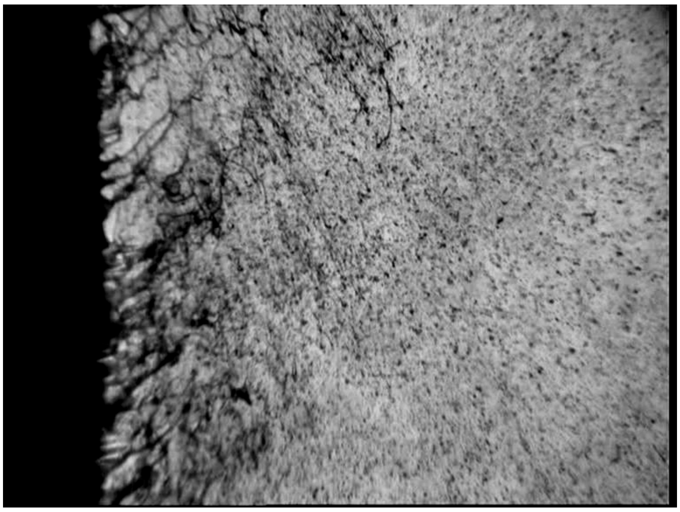

Figure 13: Jet disintegration process at bell edge (no serrations at bell edge, 40 000 1/min)

In the transition mode, the correlation between Sauter mean diameter and atomizer and fluid properties is defined by Equation 3 [6]

$$D_{32} = 0.034 \cdot We^{-0.47} \qquad (3)$$

with the We-number based on the bell speed and the bell diameter:

$$We = \frac{\pi^2 D^3 n^2 \rho_L}{\sigma} \qquad (4)$$

As indicated by Fig. 14, theoretical and experimental Sauter mean diameters are in good agreement. The measurements are made using a SPRAYTEC Fraunhofer diffraction instrument with its measurement volume being located at a typical distance of 10 mm from the bell edge. Obtained differences are below 1 µm, which is, according to the reproducibility of the measurements, not significant.

In general, the Sauter mean diameters are in the range of 10 µm, denoting a very effective atomization process leading to small fine droplets even for paint with a viscosity of 80 mPas. This is consistent with Equation 3, in which the Re-number and, hence, the viscosity of paint does not appear. Obviously, there is some excess energy available due to the high speed of the bell, eliminating the effect of the viscosity and, in the range considered, also the effect of the paint flow rate.

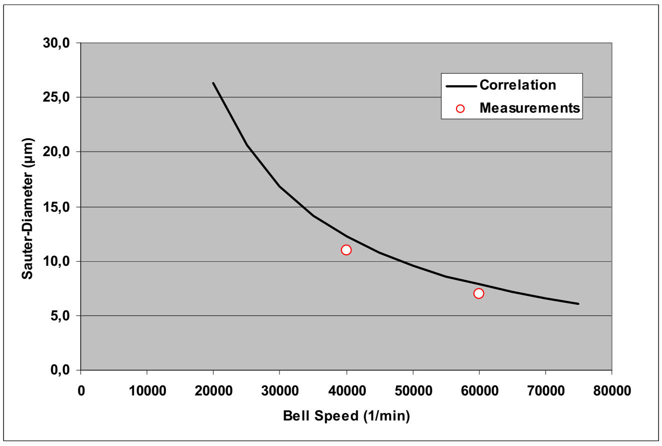

Figure 14: Comparison between theoretical and measured Sauter mean diameters (no serrations)

In Fig. 15, the measured volume weighted size distributions of serrated and non-serrated bells at a bell speed of 40 000 1/min are compared. In contrast to the expectations induced by the different disintegration figures, the widths of the size distributions are quite similar. Moreover, the serrated bell delivers a bimodal size distribution, which might be the result of some imperfections of the serration geometry. In any case, the purpose of serrations to achieve specifically narrow size distributions could not be realized. The Sauter mean diameters of both bell geometries are also very similar.

Local film thicknesses and flow field properties at the bell edge provide appropriate initial conditions for a subsequent calculation of jet formation and disintegration, which is, in this case, extremely well organized. Hence, it might be sufficient to calculate a limited number of jets only to estimate the produced droplet size distribution.

CONCLUSIONS

Although some research work dealing with high-speed rotary bell atomizers has been done in the past years, knowledge on the very specific and complicated two-flow field between the nozzle exit, the gap between the distributor disk and the bell and the emerging film on the inner bell surface is still quite limited. However, due to the complexity of the liquid flow emerging from the nozzle and hitting the surface of the distributor disk, there is a potential risk of bubble inclusion in the liquid, causing visible failures in the final coating film. Here, it should be noted, that the paints exhibit relatively high viscosities, hindering a fast degassing of the liquid.

As presented in this paper, numerical simulations based on the VOF method in the CFD code FLUENT are able to provide basic results concerning the behavior of the paint flow emerging from the nozzle and propagating along the surfaces of the distributor disk and the bell itself. Well defined interface structures between liquid and gas could be calculated and some regions could be defined, in which a stronger mixture between gas and paint flow occurs. These regions might be the source of gas bubbles which are further transported downstream by the paint flow and included in some bigger droplets. Finally, these bubbly laden droplets lead to failures in the paint film on the substrate.

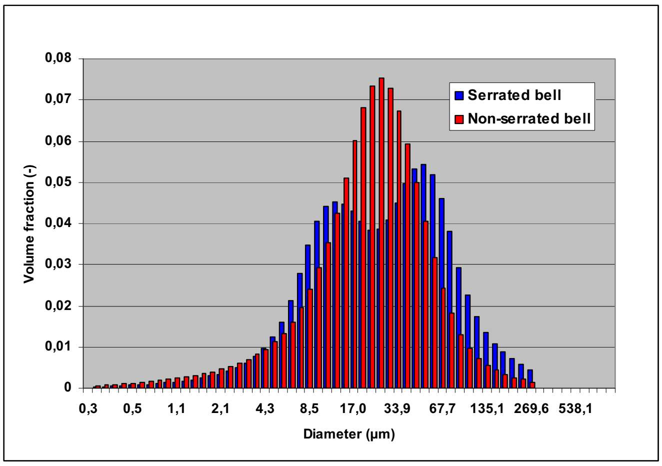

Figure 14: Comparison of measured volume size distributions for serrated and non-serrated bell (speed 40 000 1/min)

Based on the numerical results, some first suggestions for improvements in the atomizer geometry have been made such as variations of the paint nozzle diameter or modifications of the shape of the distributor disk. Clearly, additional calculations with a further increased spatial resolution in interesting regions would be required to see any real evidence of bubble formation.

Apart from this very specific task of detecting a potential risk for bubble formation, the results shown here may also serve as a basis for future calculations of the droplet formation. The presented calculations deliver detailed information on film thickness and film velocity depending on the local geometry of the bell edge proving all necessary data for the onset of disintegration calculations.

ACKNOWLEDGMENTS

The authors would like to thank the steering committee for the provision of computation time at the supercomputing facilities of the Höchstleistungsrechenzentrum (HLRS) Stuttgart, Germany.

NOMENCLATURE

Symbol	Quantity	SI Unit
D	Bell diameter	m
F	Force	N
g	Gravity	m/s²
n	Bell speed	1/min
p	Pressure	N/m²
t	Time	s
v	Velocity	m/s
We	Weber-number	-
α	Void fraction	-
ρ	Density	kg/m³
μ	Dynamic viscosity	Pa s
σ	Surface tension	N/m

REFERENCES

[1] P. L. Corbeels, D. W. Senser, A. H. Lefebvre: Atomization characteristics of a high-speed rotary-bell paint applicator. Atomization and Sprays 1992, 2, 87-89.

[2] J. Domnick, A. Scheibe and Q. Ye: The simulation of the electrostatic spray painting process with high-speed rotary bell atomizers. Part I: Direct Charging. Part. & Part. Syst. Charact. 22 (2005) 141-150.

[3] J. Domnick, A. Scheibe and Q. Ye: The simulation of the electrostatic spray painting process with high-speed rotary bell atomizers. Part II: External Charging. Part. & Part. Syst. Charact. 23(2006) 408-416.

[4] Fluent 6.2 User Manual.

[5] L. Bayvel, Z. Orzechowski; Liquid Atomization, Taylor & Frances Publishing, 1993

[6] J. Domnick, M. Thieme: Atomization Characteristics of High-speed Rotary Bell Atomizers, Atomization and Sprays, Vol. 16, No.8, (2006) 857-874